JOURNAL OF SOLID STATE CHEMISTRY 110, 176–179 (1994)

Orthorhombic–Tetragonal and Semiconductor–Metal Transitions in the $La_{1-x}Sr_xRhO_3$ System

T. A. Mary and U. V. Varadaraju

Materials Science Research Centre, Indian Institute of Technology, Madras 600 036, India

Received July 26, 1993; accepted August 23, 1993

Systematic studies of the $La_{1-x}Sr_xRhO_3$ system reveal that single phase formation exists up to $x = 0.4$. The structure undergoes an orthorhombic to tetragonal transition at $x = 0.4$. A semiconducting to metal transition occurs at $x = 0.3$. All the phases show paramagnetic behavior. © 1994 Academic Press, Inc.

INTRODUCTION

The recently discovered ceramic copper-based mixed oxides which show high T_c superconductivity have perovskite-related layer-type structure. The common features of almost all the known oxide superconductors (both low and high T_c) are that they always exhibit mixed valency ($Cu^{2+/3+}$, $O^{2-/1-}$, $Ti^{3+/4+}$, $Bi^{3+/5+}$) and that they all have insulating parent compounds and superconductivity is encountered in the metallic side of the semiconductor/metal phase boundary. In oxide superconductors, the transition from semiconducting to metallic behavior is encountered as a function of either the oxygen content of the compound or that of the dopant concentration at the counter cation site. The induction of mixed valency and semiconductor–metal phase boundary can be used as a guideline to search for new oxide superconducting materials.

The perovskite structure of a mixed oxide system is conducive to the occurrence of superconductivity (e.g., $BaPb_{1-x}Bi_xO_3$, $K_xBa_{1-x}BiO_3$, Rb_xWO_3, Cs_xWO_3, and $YBa_2Cu_3O_7$). Following the above guidelines for search for superconductivity, we have selected the $La_{1-x}Sr_xRhO_3$ system where the parent phase $LaRhO_3$ has a perovskite structure with Rh in 3+ oxidation state and exhibits semiconducting behavior. The strategy is to make it metallic by Sr doping at the La site and thereby induce mixed valency at the Rh site (Rh^{3+}/Rh^{4+}), and search for superconductivity.

EXPERIMENTAL

The following compositions have been synthesized and studied: $La_{1-x}Sr_xRhO_3$, $x = 0.0, 0.2, 0.25, 0.3, 0.33, 0.4, 0.5$. The phases are prepared by the conventional high temperature solid state reaction. High purity starting materials are used: La_2O_3 (99.9%, IRE, India; preheated at 950°C and kept in a desiccator), $SrCO_3$ (99.99%, Cerac), and Rh_2O_3 (prepared by dissolving Rh metal powder (99.99%, Alfa Products, Germany) in concentrated HNO_3, evaporating the nitrate cake over a water bath, decomposing above 600°C, and sintering at 1000°C. The phase is characterized by powder XRD technique). Stoichiometric amounts of the oxides are ground well in an agate mortar and the mixed powder is heated in a platinum crucible at 1100°C for 48 hr with intermediate grindings. The reacted powder is then pressed into pellets and heated for another 48 hr at 1100°C and furnace cooled. Select phases are given oxygen treatment at 350°C for 5 days and furnace cooled in flowing oxygen.

The compounds are characterized by powder X-ray diffraction (Seifert Unit; Cu$K\alpha$ radiation). The lattice parameters are calculated by LSQ fitting of high angle reflections. Four probe dc electrical resistivity (ρ) studies, as a function of temperature in the range 300–13 K, are done by van der Pauw method on well-sintered pellets using a closed cycle He refrigerator (CTI-Cryogenics, model M22). The electrical contacts are given by conducting silver paint. A Keithley nanovoltmeter (Model 181) and a dc constant current supply (10 mA) are employed for the measurements. Magnetic susceptibility studies are done using a SQUID magnetometer (Quantum Design, Model 1822, MPMS) on select samples in the range 300–4.2 K in a field of 100 G.

RESULTS AND DISCUSSION

(a) Structure and Stoichiometry

The compounds are black in color and are stable toward exposure to atmosphere. The XRD patterns reveal well-crystallized single phase formation for phases with $x = 0.0$–0.4 (Fig. 1). The XRD pattern of the $La_{0.5}Sr_{0.5}RhO_3$ phase shows additional peaks due to impurities. The undoped $LaRhO_3$ phase has an orthorhombic structure and the lattice parameters (Table 1) are in good agreement with the values reported in the literature (1).

0022-4596/94 $6.00

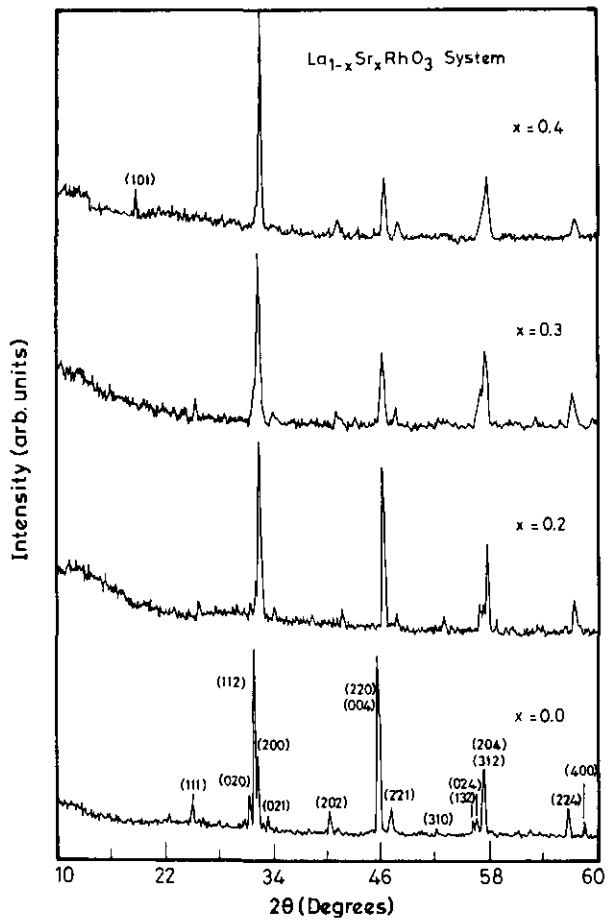

FIG. 1. XRD patterns for the $La_{1-x}Sr_xRhO_3$ system indicating an O–T transition at $x = 0.4$.

As the Sr content increases, the a-axis increases and the b-axis decreases, resulting in an orthorhombic–tetragonal (O–T) transition at $x = 0.4$. The O–T transition is evident from the merging of the (020, 200), (132, 312), and (024, 204) peaks in the X-ray patterns (Fig. 1). In $LaRhO_3$, since the tolerance ratio is less than 1 ($t = 0.8$), the RhO_6 octahedra tilt as in the $GdFeO_3$ structure. When larger Sr^{2+} are substituted at the La^{3+} site (1.46 vs 1.34 Å for 12-fold coordination), the tolerance factor increases and hence the orthorhombic distortion decreases and the structure becomes tetragonal for $x = 0.4$. The c-axis remains more or less constant. However, the unit cell volume decreases slightly as a function of Sr content. The relative effect of conversion of Rh^{3+} to smaller Rh^{4+} in the B sublattice of the perovskite structure dominates over the effect of substitution of larger Sr^{2+} for smaller La^{3+}.

While this manuscript was under preparation, we came across a recent report on preparation and properties of $La_{1-x}M_xRhO_3$ (M = Ca, Sr, Ba) by Nakamura et al. (2). They have observed single phase formation only up to $x = 0.1$ for M = Sr. They have employed a sintering temperature of 1250°C. Initially, we also sintered the pellets at 1200–1300°C and found that the compounds are multiphasic. It is reported that Rh_2O_3 decomposes above 1100°C (3). Hence, the low solid solubility observed by Nakamura *et al.* (2) could be due to the high sintering temperature employed.

(b) Electrical Properties

The room-temperature resistivity of $LaRhO_3$ is 3.5 Ω cm (Table 1) and it exhibits a semiconducting behavior at low temperatures (Fig. 2a). The E_a value for $LaRhO_3$ is 0.06 eV (from the Arrhenius equation) in the temperature range 300–100 K. Our $\rho_{300\,K}$ and E_a values are in contrast with those reported earlier for $LaRhO_3$. Bouchard *et al.* (4) have reported the $\rho_{300\,K}$ of $LaRhO_3$, measured by two-probe method, as $\sim 10^4$ Ω cm. Shaplygin and Lazarev (5) have reported the $\rho_{300\,K}$ of $LaRhO_3$ as 8×10^3 Ω cm. However, recently, Nakamura *et al.* (2), from a systematic measurement of resistivity by four-probe method, report the $\rho_{300\,K}$ as ~45 Ω cm. The $\rho_{100\,K}$ observed in the present study as well as in Ref. (2) are in good agreement ($\sim 10^4$ Ω cm).

As the Sr content increases the electrical resistivity decreases and a semiconductor–metal transition occurs (Figs. 2a and 2b). Phases with $x = 0.2$ and 0.25 exhibit semiconducting behavior down to 13 K (limit of our measurement). The E_a values also decrease as Sr content

TABLE 1
Structural, Electrical, and Magnetic Data for the $La_{1-x}Sr_xRhO_3$ System

x	Lattice parameter (Å) a	b	c	$(b-a)/a \times 10^{-2}$	V (Å^3)	$\rho_{300\,K}$ (Ω cm)	E_a (eV) (300–100 K)	$\chi_{300\,K} \times 10^{-4}$ (emu/mole/G)
0.00	5.53	5.70	7.90	3.07	249	3.50	0.06	1.44
0.20	5.54	5.66	7.89	2.17	247	0.47	0.02	2.30
0.25	5.55	5.67	7.89	2.16	248	0.085	0.007	2.23
0.30	5.54	5.65	7.89	1.99	247	0.024	—	—
0.33	5.55	5.66	7.92	1.99	249	0.022	—	3.69
0.40	5.57	5.57	7.89	0.0	245	0.025	—	3.10
0.50	5.59	5.59	7.90	0.0	247	0.056	—	—

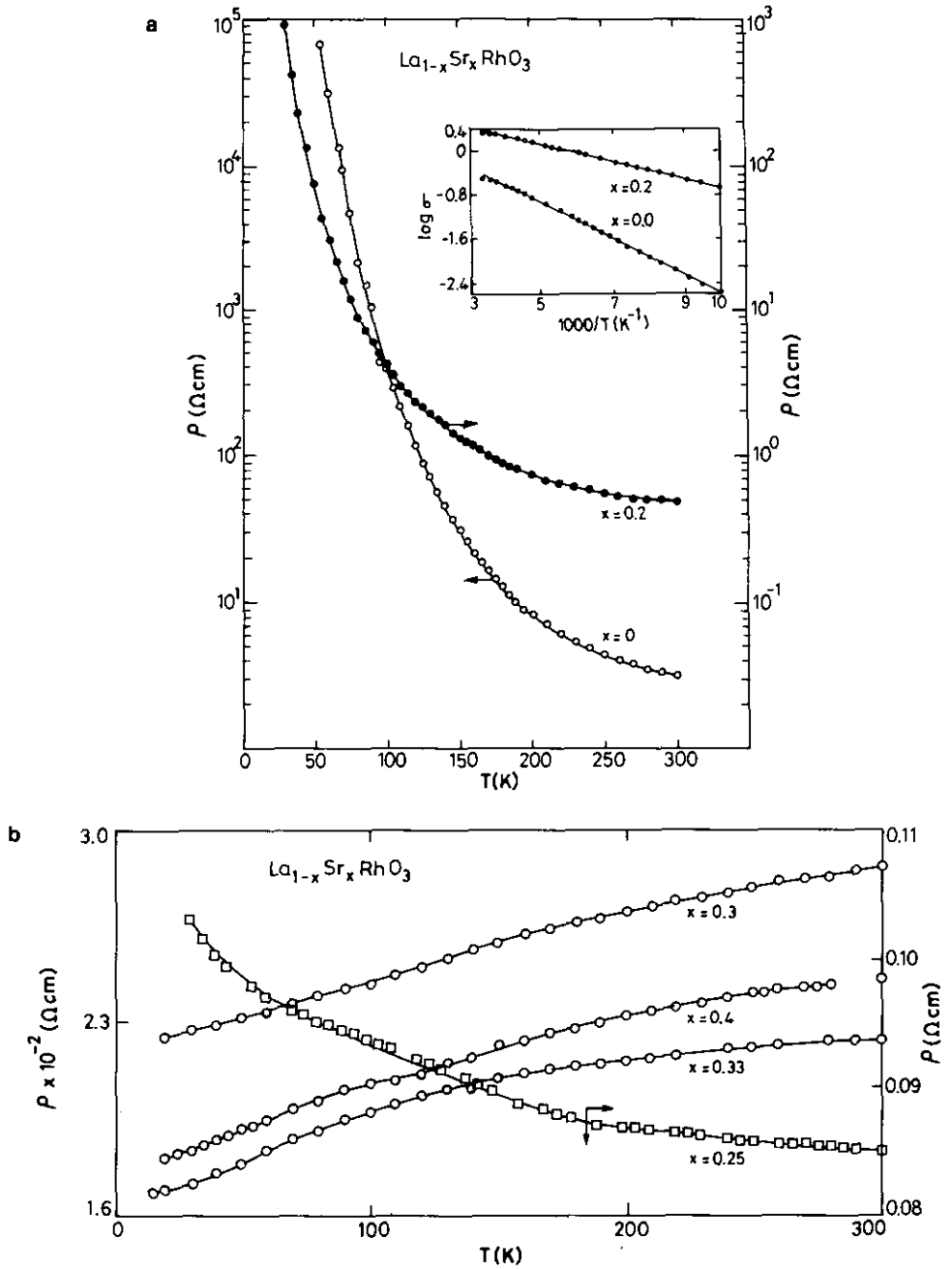

FIG. 2. (a-b) ρ vs T plots for the $La_{1-x}Sr_xRhO_3$ system. Inset in (a) shows the log σ vs $1000/T$ plots.

increases. The semiconductor–metal transition occurs at $x = 0.3$. Phases with $x = 0.3, 0.33$, and 0.4 exhibit metallic conductivity down to 13 K. $\rho_{300\,K}$ decreases from $x = 0.3$ to $x = 0.33$, but the $x = 0.4$ phase exhibits a slightly higher resistivity than that of the $x = 0.33$ phase and the $x = 0.5$ phase shows semiconducting behavior probably due to the presence of impurities. The $\rho_{300\,K}$ and the ρ–T behavior of the oxygen annealed phases are exactly in agreement with the values for the corresponding air heated phases, confirming that the air heated samples are not oxygen deficient. No superconductivity is encountered in any of the phases. Recently Nakamura *et al.* (2) also observed a decrease in resistivity as Sr content increases. However, they do not encounter metallicity due to the low solid solubility of Sr.

The electrical properties of $LaRhO_3$ can be explained based on Goodenough's one electron band model for perovskite oxides (6). For the $3d$ transition elements the correlation energy is large and the electrons in the d bands tend to localize. For the $4d$ transition elements, correlation energy and hence localization is much reduced. The spatial extension of the $4d$ shell is larger than that of a

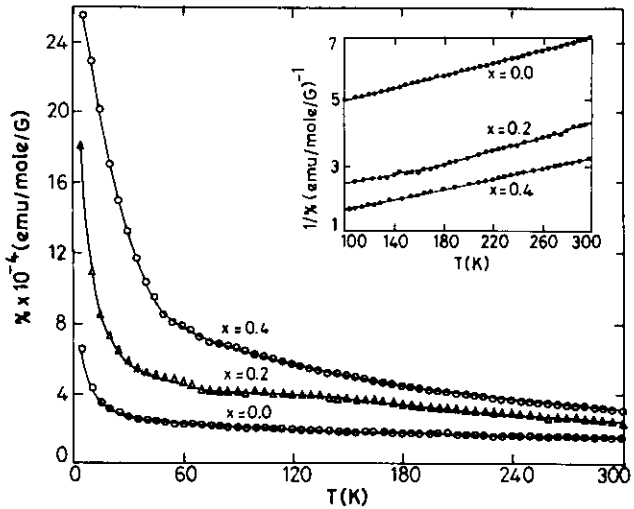

FIG. 3. χ vs T plots for the $La_{1-x}Sr_xRhO_3$ system. Inset shows the $1/\chi$ vs T plots.

3*d* shell. Hence, for 4*d* elements, filled *d* bands or subbands are more likely to form extended states with an intermediate range of hole mobility (7). In $LaRhO_3$, Rh^{3+} is in an octahedral crystal field of six oxygen anions. In such a crystal field, the e_g orbitals are separated from t_{2g} orbitals by a band gap. The six 4*d* electrons from Rh^{3+} occupy the t_{2g} subshell. Excitation of electrons from the filled t_{2g} level to the empty e_g level creates holes in the t_{2g} level and hence, electrical conductivity is effected. Substitution of Sr^{2+} for La^{3+} creates an equivalent amount of Rh^{4+} ($4d^5$) in the lattice for charge compensation. The increase in conductivity is due to the creation of more and more holes in the t_{2g} band.

(c) Magnetic Properties

The undoped $LaRhO_3$ is found to exhibit a temperature dependent paramagnetic behavior (Fig. 3). The inverse susceptibility varies linearly with temperature in the range 300–100 K (inset Fig. 3) showing Curie–Weiss behavior with low effective magnetic moment (μ_{eff} = 0.9 BM) for the rhodium ion. $\chi_{300\,K}$ increases as Sr content increases. Even the metallic phases exhibit paramagnetic behavior instead of the expected temperature-independent Pauli paramagnetism. The effective magnetic moment is around 0.9 BM for all the Sr doped phases. It is reported that *p*-type $LuRhO_3$ shows almost temperature-independent paramagnetism in the range 300–77 K and paramagnetic behavior in the range 70–5 K (8). Sr_2RhO_4 also exhibits paramagnetic behavior (9), whereas temperature-independent susceptibility would have been expected from the metallic nature of the sample. The magnetic behavior of Sr_2RhO_4 is explained as being due to an ordering of magnetic moments. Indeed, pure Rh_2O_3 (Rh^{3+}; d^6 ion) exhibits temperature-independent paramagnetism instead of diamagnetism, and this is due to the presence of a small amount of Rh^{4+} in the Rh_2O_3 (3).

CONCLUSIONS

In the present study on the $La_{1-x}Sr_xRhO_3$ system, solid solubility up to 40 atom% of Sr is established. The occurrence of the O–T transition at $x = 0.4$ and the semiconducting–metal transition at $x = 0.3$ proves that Sr is indeed substituted at the La site and a mixed valency is created at the Rh site (Rh^{3+}/Rh^{4+}).

REFERENCES

1. A. Wold, B. Post, and E. Banks, *J. Am. Chem. Soc.* **79,** 6365 (1957).
2. T. Nakamura, T. Shimura, M. Itoh, and Y. Takeda, *J. Solid State Chem.* **103,** 523 (1993).
3. H. Leiva, R. Kershaw, K. Dwight, and A. Wold, *Mater. Res. Bull.* **17,** 1539 (1982).
4. R. J. Bouchard and J. F. Weiher, *J. Solid State Chem.* **4,** 80 (1972).
5. I. S. Shaplygin and V. B. Lazarev, *Russ. J. Inorg. Chem. Engl. Transl.* **25,** 1769 (1980); V. B. Lazarev and I. S. Shaplygin, *Russ. J. Inorg. Chem. Engl. Transl.* **23,** 163 (1978).
6. J. B. Goodenough, "Progress in Solid State Chemistry" (H. Reiss, Ed.), Vol. 5, p. 231. Pergamon, New York, 1971.
7. J. B. Goodenough, *J. Appl. Phys.* **37,** 1415 (1966).
8. H. S. Jarrett, A. W. Sleight, H. H. Kung, and J. L. Gillson, *J. Appl. Phys.* **51,** 3916 (1980).
9. T. Shimura, M. Itoh, and T. Nakamura, *J. Solid State Chem.* **98,** 198 (1992).